Published in final edited form as:
Hepatology. 2013 November ; 58(5): 1693–1702. doi:10.1002/hep.26540.

Identification of Driver Genes in Hepatocellular Carcinoma by Exome Sequencing

Sean P. Cleary[1], **William R. Jeck**[2,3], **Xiaobei Zhao**[2,3], **Kui Chen**[1], **Sara R. Selitsky**[2,3], **Gleb L. Savich**[2,3], **Ting-Xu Tan**[2,3], **Michael C. Wu**[4], **Gad Getz**[5], **Michael S. Lawrence**[5], **Joel S. Parker**[3], **Jinyu Li**[6], **Scott Powers**[6], **Hyeja Kim**[1], **Sandra Fischer**[7], **Maha Guindi**[7,8], **Anand Ghanekar**[1], and **Derek Y. Chiang**[2,3]

[1]Department of Surgery, University Health Network, University of Toronto, Toronto, Canada

[2]Department of Genetics, University of North Carolina, Chapel Hill, NC 27599

[3]Lineberger Comprehensive Cancer Center, University of North Carolina, Chapel Hill, NC 27599

[4]Department of Biostatistics, University of North Carolina, Chapel Hill, NC 27599

[5]Genome Sequencing Analysis Program and Platform, Broad Institute, Cambridge, MA 02142

[6]Cold Spring Harbor Laboratory, Cold Spring Harbor, NY 11724

[7]Department of Pathology, University Health Network, University of Toronto, Toronto, Canada

[8]Department of Pathology, Cedars-Sinai Medical Center, Los Angeles, CA 90048

Abstract

Genetic alterations in specific driver genes lead to disruption of cellular pathways and are critical events in the instigation and progression of hepatocellular carcinoma. As a prerequisite for individualized cancer treatment, we sought to characterize the landscape of recurrent somatic mutations in hepatocellular carcinoma. We performed whole exome sequencing on 87 hepatocellular carcinomas and matched normal adjacent tissues to anaverage coverage of 59x. The overall mutation rate was roughly 2 mutations per Mb, with a median of 45 non-synonymous mutations that altered the amino acid sequence (range 2 to 381). We found recurrent mutations in several genes with high transcript levels: *TP53* (18%), *CTNNB1* (10%), *KEAP1* (8%), *C16orf62* (8%), *MLL4*(7%) and *RAC2* (5%). Significantly affected gene families include the nucleotide-binding domain and leucine rich repeat containing family, calcium channel subunits, and histone methyltransferases. In particular, the *MLL* family of methyltransferases for histone H3 lysine 4 were mutated in 20% of tumors.

Conclusion—The *NFE2L2-KEAP1* and *MLL* pathways are recurrently mutated in multiple cohorts of hepatocellular carcinoma.

Keywords

HCC; mutations; histone methyltransferases

INTRODUCTION

Hepatocarcinogenesis is instigated by copy number alterations, mutations and chromosomal rearrangements that activate oncogenes or inactivate tumor suppressors. Previous genetic

Corresponding Author: Derek Chiang, PhD, Lineberger Comprehensive Cancer Center, University of North Carolina, 450 West Drive, CB #7295, Chapel Hill, NC 27599-7295, Tel: (919) 843-7887, Fax: (919) 966-3015, chiang@med.unc.edu.

characterization of hepatocellular carcinoma (HCC) has indicated significant heterogeneity among tumors, which has hampered the development of targeted therapy. Genomic and transcriptomic profiling studies have attempted to classify tumor molecular subgroups and have implicated several signaling pathways that are mutated in HCC (1–3). The Wnt β-catenin signaling pathway members, *CTNNB1*, *AXIN1* and *AXIN2* are collectively mutated in up to half of tumors. The most frequently mutated tumor suppressor is *TP53*, which has mutations in over 20% of tumors. Over half of hepatocellular carcinomas harbor gains of chromosome 1q and 8q, which include candidate oncogenes *MCL1*, *SHC1*, *MYC* and *COPS5*/*JAB1*, among hundreds of other genes(4–8).

To date, studies of the mutational spectrum of HCC have focused on a limited number of candidate genes. Advances in genome sequencing technologies have enabled the simultaneous analysis of thousands of expressed genes accelerating the search for additional novel and recurrently mutated genes (9–14). Recent studies have identified the ATP-dependent nucleosome remodeling enzymes, *ARID1A* and *ARID2*, to be mutated in approximately 15% and 5% of tumors, respectively (11–14). A regulator of the redox signaling pathway, *NFE2L2*, is mutated in 6% of tumors (12). Other genes mutated at greater than 3% frequency include *RPS6KA3*, *IL6ST*, *NRAS*, *KRAS*, *PIK3CA*, *PTEN*, *SAMD9L*, *DMXL1* and *NLRP1*(11, 13, 15).

The genetic heterogeneity of HCC has complicated our understanding of the molecular basis of this disease. In order to further define theimportant recurrent and clinically actionablemutations in HCC, we embarked on a large-scale study of 87 tumors that was powered to detect mutated genes at a population prevalence of at least 10%. We hypothesized that multiple component genes of certain signaling pathways could be recurrently mutated in hepatocellular carcinoma.

EXPERIMENTAL PROCEDURES

Human subjects

Subjects were identified and informed consent was obtained from consecutive patients undergoing surgical resection for confirmed HCC at the University Health Network (Toronto, Canada) and the University of North Carolina. Five additional tumor specimens were procured from the Cooperative Human Tissue Network. All surgical specimens were processed according to established institutional HCC-tumor banking protocols. In brief, fresh surgical specimens underwent immediate gross pathologic examination by experienced liver pathologists. Samples were obtained from viable tumor and non-tumor liver >2 cm away from the primary lesion. Tumors with evidence of prior therapy, such as radiofrequency ablation or trans-arterial chemo-embolization were excluded. Tissue samples were bisected with half of the tissue stored in liquid nitrogen and the mirror sample retained for histologic confirmation. All tumor samples were histologically assessed for diagnosis and cellularity and non-tumor liver samples were confirmed to be free of tumor cells.

DNA extraction and sequencing libraries

Tissue samples were thawed and weighed prior to homogenization. Genomic DNA and RNA was extracted with the Qiagen AllPrep kit (Valencia, CA) and quality was assessed on 2% agarose gel. Genomic DNA for exome capture and sequencing was prepared using either SureSelect Target Enrichment System for Illumina Paired-End Sequencing Library (Agilent Technologies, Santa Clara, CA) according to manufacturer's instructions (protocol versions 1.2, May 2011 and 1.3.1, February 2012) or equivalent enzymes (New England Biolabs, Ipswich, MA) and Agilent's protocol (version 2.0.1, May 2010). Briefly, 2–3 micrograms of genomic DNA were sheared on Covaris S220 (Woburn, MA) to 150–200 bp target size with

the following instrument settings: 10% duty cycle; intensity 5; 200 cycles per burst; 6 cycles of 60 seconds each in frequency sweeping mode. Sheared fragments were ligated to Illumina's adapters and enriched by 5–6 cycles of amplification. Five hundred nanograms of amplified libraries were incubated with Agilent's whole exome capture oligos for 24h at 65°C. Hybridized fragments were captured with streptavidin-coated beads, eluted, and amplified by 10–12 cycles of PCR utilizing either one of 12 Agilent's indexed primers or not indexed SureSelect GA PCR primers). Prepared libraries were pooled in batches of 4 and sequenced on Illumina HiSeq 2000 (San Diego, CA) instrument generating 100 bp paired end reads. Alternatively, individual libraries were sequenced on Illumina GAII instrument generating 76 bp paired end reads.

We enriched for protein coding regions with the Agilent AllExon version 1 sequence capture baits for 10 tumors and matched normals, and with the Nimblegen Human exome version 1 sequence capture baits for 5 tumors and matched normals. These captured libraries were sequenced on the Illumina Genome Analyzer II to an average of 4.8x and 5.8x, respectively. An additional 72 tumors and matched normals were captured on the Agilent AllExon version 4 sequence capture baits, and sequenced in pools of 4 samples with the IlluminaHiSeq 2000 to an average of 59x coverage (Supplementary Figure 1).

Bioinformatics sequence analysis

Sequences were mapped to the human genome (NCBI37/hg19), excluding alternative haplotype chromosomes, using the Bowtie 2 alignment algorithm (16). Alignments were refined using The Genome Analysis ToolKitto mark PCR duplicate reads and perform base quality recalibration(17, 18). Alignments from each tumor and matched normal were then analyzed by the MuTect algorithm(19, 20). In brief, MuTect includes a preprocessing step for sequence read qualities, a Bayesian classifier to assess the posterior probability of somatic mutations, and post-processing of candidate mutations. Somatic mutations were assigned to transcript and amino acid coordinates using the ANNOVAR software suite(21).

Availability of genetic sequencing data

Binary sequence alignment map files (BAM files) have been deposited in the National Center for Biotechnology Information dbGAP database.

Significantly mutated genes and pathways

The MutSig software version 1.5 identified the list of significantly mutated genes among 87 hepatocellular carcinomas (20)(https://confluence.broadinstitute.org/display/CGATools/MutSig). Genes that harbored a greater number of mutations than expected by chance were detected with a binomial test. For each gene, the observed number of mutations across the 87 tumors was compared to the expected number based on the background mutation rates and the covered bases in all samples. The binomial probabilities were adjusted to False Discovery Rate *q*-values with the Benjamini-Hochberg procedure and reported in Table 1.

Gene families were downloaded in May 2012 from the HUGO Gene Nomenclature Committee database (22)(http://www.genenames.org/genefamilies/a-z). For each gene family, we tested for an enrichment of mutations in the genes within the family relative to the genes outside of the family. For each individual, we calculated the per-base mutation rate among the exons of the genes within the gene family and among the exons of the genes outside of the gene family. We then tested whether the average mutation rate within a gene family was higher than the average mutation rate for genes outside the family using a one-sided, paired *t*-test.

RNA Isolation from Tissue samples and Quantitative Real-time PCR

Total RNA was prepared using Qiagen AllPrep kit (Qiagen, Valencia, CA) and quality was assessed on 2% agarose gel. MVP™ Human Liver Total RNA pool (Agilent Technologies, Santa Clara, CA) was introduced as a standard control. cDNA was synthesized using 200ng random primers (Thermo Scientific, Rockford, IL) and 200U M-MLV Reverse Transcriptase (Life Technologies, Grand Island, NY) from 2μg of each total RNA sample according to the manufacturer's instructions. All samples within an experiment were reverse transcribed under the same condition, the resulting cDNA diluted 1:5 in nuclease-free water and stored in aliquots at −20°C until used. Real-time PCR with SYBR green detection was performed in Light Cycler 480 System (Roche Applied Science, Indianapolis, IN) in a total reaction volume of 20 μL in 384-well plate. Each reaction contained 5μL of diluted cDNA, 500nM of each primer (as listed in Supplementary Table 1) and 1× LightCyclerR 480 SYBR Green I master mix. The real-time PCR running protocol consisted of (1) 5 min pre-incubation at 95°C; (2) amplification (10 s at 95°C; 10 s at 60°C; 15 s at 72°C); (3) melting curve (10 s at 95°C, 65–97°C at at 2.5°C/s –1 and a continuous fluorescent measurement); and (4) 10 s cooling at 40°C. Relative quantitative analysis was carried out according to the $2^{-\Delta\Delta Ct}$ method(23).

Statistical analyses

Descriptive characteristics of genetic and clinical variables were reported as frequencies and percentages for categorical variables; continuous variable were reported as medians and range. Comparisons of frequencies between genetic and clinical variables were performed using chi-square and Fisher's exact test, where appropriate. Survival analyses were performed using the Kaplan-Meier method. Univariate survival analysis was performed using the Log-rank tests and multivariate analyses conducted using Cox proportional hazards model.

RESULTS

Clinical characteristics of HCC specimens

Complete clinical data was available for 87 of 89 (98%) tumor samples and is shown in Table 1. Cases included a mix of predisposing disease etiologies including 43% and 21% of patients with hepatitis B and C, respectively. Nineteen cases had multifocal disease at the time of surgery, however only one tumor was submitted for analysis in each case. Positive staining for CK19 in >5% of cells was seen in 12 cases and 2 tumors were fibrolamellar HCC. Median follow-up of cases was 33.8 months (range 3–130 months). There were 3 (3.8%) perioperative deaths within 90 days. A total of 28/87 (32%) patients died with a mean overall survival of 80.6 months with a 5-year overall survival estimated at 76% by Kaplan-Meier analysis. During follow-up there were a total of 44 recurrences for a median disease-free survival of 39.1 months.

Significantly mutated genes in HCC cohort

In total, we found 5820 non-synonymous mutations and 433 nonsense mutations in these 87 tumors (average 66.1, range 4 to 362) or 2.5 mutations per Mb sequenced (Figure 1A). The somatic mutation rate is comparable to those reported in previous studies (11–14). The mutational bias for CpG to A/T transversions in hepatocellular carcinoma was consistent with previous studies (Figure 1B).

We followed standard statistical analyses to discriminate driver mutations from random mutations (19, 24). We assumed that most of the mutations in cancer genomes represent background noise, while driver genes would be mutated more frequently than expected by chance. We used a binomial probability to estimate the expected number of mutations for

each sample. This probability distribution corrects for gene length, due to the assumption that longer genes will be expected to accumulate more mutations by chance. We calculated the background mutation rate using all of the nonsynonymous and synonymous mutations determined in all 87 samples. For each mutated gene, we then calculated the binomial probability of observing at least *N* mutations, given the background mutation rate. The *p*-value was adjusted for multiple hypotheses using the Benjamini-Hochberg procedure for controlling False Discovery Rate (FDR). In this analysis, we identified 34genes that were significantly mutated from the discovery cohort, according to a False Discovery Rate cutoff of 10%.

The most frequently mutated genes in this cohort were the well-known oncogene *CTNNB1* (10%) and tumor suppressor, *TP53* (18%)(Table 2). *CTNNB1* mutations and activation of the *Wnt* pathway have been associated with large (>3cm) tumors, poorly differentiated histology, tumor invasion and metastases as well as HCV-associated HCC. *TP53* mutations have been associated with all predisposing etiologies with specific Ser249 mutations associated with Aflatoxin B exposure. *KEAP1*, encoding kelch-like ECH-associated protein 1, retains *NFE2L2*/*NRF2* in the cytosol and regulates the Keap1-Nrf2 cell defense pathway (25). Previous studies have showed that the Keap1-Nrf2 signaling pathway mediates protective cellular responses to oxidative and xenobiotic damage (26, 27). The roles of *IGSF3*, *ATAD3B* and *PCMTD1* have not been previously characterized in HCC.

Significant enrichment of mutations in histone methyltransferases

To further characterize the pattern of mutated genes and explore their significance of functional pathways in HCC, we analyzed mutations within known gene families (Table 3). Among 4 histone H3 lysine 4 methyltransferases of the *MLL* family, we validated 13 missense mutations by PCR and Sanger-based resequencing. We identified 2 tumors with *MLL* mutations, 4 tumors with *MLL2* mutations, 1 tumor with *MLL3* mutations and 6 tumors with *MLL4* mutations (Figure 2A to 2D). Among the *MLL* gene family, the *MLL2* and *MLL4* genes seem to be the most likely driver genes in HCC. *MLL4* encodes mixed lineage leukemia-4, one of the *MLL* family of histone H3 lysine-4 (H3K4)-specific methyl transferases. Notably, *MLL4* is a recurrent hotspot for hepatitis B virus integration in nearly 12% of hepatocellular carcinoma genomes (28). *MLL3* and *MLL4* participate in transcriptional coactivator complexes and are necessary for the expression of p53 target genes in response to DNA damage (29). Knockdown of *MLL4* reduces cell cycle progression and induces apoptosis (30).

Transcript levels of recurrently mutated genes

We further sought to confirm expression level signatures of 13 recurrently mutated genes in tumor and liver samples used for sequencing analysis. Total RNA was extracted from 49 tumor samples, 8 non-tumor liver samples from HCC patients and normal liver reference RNA. Among the tumors selected for expression analysis, 39 had mutations in recurrently altered genes, 10 tumors lacked mutations in the genes of interest. In the non-tumor liver specimens of HCC cases overexpression of several genes was observed including *TP53* (6/8 samples), *CTNNB1* (4/8), *ATAD3B* (5/8), *PCMTD1* (5/8), *BRD9* (4/8), *TTLL2* (4/8), *TMEM170A* (4/8), *TMEM51* (5/8) and *GJA1* (3/8), while *IGSF3* was underexpressed in 5/8 samples(Figure 3). Among samples with a confirmed *TP53* mutation, the gene was overexpressed in 5/9 and underexpresed in 3/9 samples. CTNNB1 was overexpressed in 7/9 tumors with mutations in this gene. KEAP1 expression levels were similar in non-tumor liver samples compared to reference controls, but decreased expression was seen in 4/6 tumors with KEAP1 mutations. Increased expression of genes in samples harbouring mutations was observed for *CPA2* (3/6 samples), *ATAD3B* (1/1), *PCMTD* (1/1), *BRD9* (5/6), *TTLL2* (2/4), *TMEM170A* (2/2), *TMEM51* (3/3) and *GJA1*(2/2).

Clinical characteristics of HCC according to mutation status

HCC arising from hepatitis C infection demonstrated a significantly higher rate of *CTNNB1* mutations (62.5% vs 37.5%, p=0.038) confirming earlier reports associating mutations in b-catenin with HCV. There was also a trend toward higher rates of microvascular invasion in HCC with *MLL* gene mutations (67% vs 45%, p=0.11). Otherwise, there were no significant associations between individual gene or gene family mutations and clinical variables assessed.

Mutations in *TP53* were associated with significantly higher rate of recurrence (89% vs 40%, p=0.006) and shorter disease-free survival (median DFS: 7.9 vs 42.9 months, p=0.001) (Figure 4). There was a trend towards decreased overall survival status among *TP53*-mutatedtumors (median OS: 26.0 vs 83.2 months, p=0.1) (Supplementary Figure 2). Tumors harboring mutations in the *MLL* family were associated with a trend toward earlier recurrence with a median disease free survival of 28.9 months for *MLL* mutation carriers compared to 45.8 months for cases without *MLL* mutations (p=0.22) and may be associated with a more aggressive disease phenotype(Supplementary Figure 3). A trend towards lower rates of recurrence (12.5% vs 49.3%, p=0.060) and prolonged disease free survival (p=0.23) was observed in cases with *CTNNB1* mutations but did not reach statistical significance due to limited power. The presence of CPA2 and KEAP1 mutations were associated with decreased disease-free survival however these analyses lacked sufficient statistical power.

Univariate analysis of disease-free survival for all clinical and genetic variables identified tumor size (p=0.042), multifocality (p=0.077), and p53 mutation status (p=0.001) as significant or borderline significant predictors of DFS(Table 4). Conditional multivariable survival analysis demonstrated that p53 mutation status was the only independent predictor of disease-free survival with a hazard ratio (HR)=4.245 (95%CI: 1.86- 9.70 (p=0.02)). Tumor multifocality was the only independent predictor of overall survival.

DISCUSSION

Hepatocellular carcinoma is a genetically heterogeneous disease; this molecular diversity has led many groups to attempt to characterize HCC to improve our understanding of the genes and pathways involved in the etiology of this disease. The goal of genomic and transcriptomic profiling efforts in HCC is to develop a molecular classification of hepatocellular carcinoma that identifies characteristic driver genes that either predict prognosis or eventually could be developed as targets for tailored therapies. This study of 87 matched tumor-normal pairs more than doubles the number of HCC characterized by whole exome sequencing, to a total of 158 tumors. Due to limited sample sizes (ranging from 10 to 27 tumors), it should not be surprising that these studies have not yielded many overlapping genes. Indeed, larger sample cohorts with clinical follow-up data will be required to discern the prognostic significance of recurrently mutated genes.

An interesting emerging consensus from these HCC sequencing studies is the prevalence of mutations in chromatin regulatory enzymes. In particular, several studies have reported mutations in the *SWI*/*SNF*-related, ATP-dependent nucleosome remodelers: *ARID1A* and *ARID2*(11–14). We only detected 2 mutations in *ARID1A*(2%) and 1 mutation in *ARID2* (1%), despite over 20x coverage of these genomic regions. However, our study concurs with recent reports of mutations in the *MLL* family of histone H3 lysine4 methyltransferases, which can also be disrupted by genomic integration of hepatitis B virus(14, 28). The clinical characteristics of tumors harboring *MLL* gene mutations suggest that inactivation of the *MLL* gene family may be associated with an aggressive tumor phenotype. However, we have not evaluated the functional impact of these mutations on histone methylation. As more data on the *MLL* gene family are collected, further studies could assess how the most frequent

mutations may impair the enzymatic function or recruitment of these enzymes. Further work is needed to elaborate how disrupted chromatin regulators cooperate with alterations in known signaling pathways – such as the Wnt/beta-catenin pathway or Myc targets – in tumor progression, cellular differentiation, or gene expression.

Woo and colleagues had previously demonstrated worse overall survival associated with p53 mutations in a cohort of predominantly Chinese HCC patients with hepatitis B virus etiology (31). This study complements those findings by demonstrating the prognostic value of HCC in a North American series of patients of mixed etiology (HBV/HCV). Combined, this data demonstrates that p53 is associated with recurrence and disease-free survival, oncologic outcomes that reflect an aspect of tumor biology, as well as overall survival, which includes death from both HCC and the underlying liver disease. The observation of p53 as an independent prognostic factor with an ability to predict outcomes in addition to tumor size and number may have important clinical implications in predicting outcomes for patients prior to treatment such as resection or transplantation.

Sorafenib represents the first molecularly targeted therapy for HCC, and the vast majority of HCC clinical trials are currently evaluating the efficacy of tyrosine kinase inhibitors (32, 33). However, the combined analysis of whole exome sequencing from 158 tumors reveals that no single protein kinase that is mutated at more than 5% frequency in hepatocellular carcinoma(9–14). This scarcity of kinase mutations suggests that HCC might be rarely susceptible to the dramatic responses to kinase inhibitors that are observed in other cancer types(34, 35). In contrast, the frequent mutation of *MLL*histone methyltransferases – as well as *ARID* ATP-dependent nucleosome remodeling enzymes identified in previous studies – suggests that epigenetic regulatory enzymes may represent important target genes in HCC.

Since most studies to date have been conducted on surgically resected tumors, we have little knowledge about the genetic alterations that occur in either very early lesions treated with ablative modalities as well as later stages of HCC progression that are not amenable to surgical treatment. Our understanding of tumor evolution could be improved by more sensitive technologies that could sequence genomic DNA from core biopsy specimens. Another confounding issue with genomic profiling is the high rate of intra-tumor heterogeneity. Indeed, a pioneering study demonstrated considerable clonal heterogeneity within a single tumor lesion, with allelic frequencies as low as 13% (10).

In this series, we present the whole-exome sequencing analysis of a large diverse series of HCC tumors and matching normal liver tissue. Our results support the genetic heterogeneity of HCC in that most genes were mutated in few (<20%) of the samples analyzed, however analysis of gene families have indicated potentially important pathways, including *MLL* and *NFE2L2-KEAP1*, that are altered in subsets of tumors. Overexpression of several genes of interest were observed in tumors with identified mutations but also in adjacent non-tumor liver samples, which suggests a role of these genes in the pre-malignant “field-effect” that is seen in the unaffected liver of HCC patients (36). We observed phenotypic differences in HCC according to gene mutation status including p53 mutation status as an independent predictor of recurrence-free survival. Several other genes of interest demonstrated trends in time and risk of recurrence; these observations were limited by sample size and require further investigation in larger studies. The lack of correlation between traditional prognostic features such as tumor size, number and vascular invasion indicates that mutational profiling may enhance our ability to develop more predictive models of tumor behavior. Further investigation is required to enhance our understanding of the full breadth of gene mutations in HCC and identify clinically-relevant genes and pathways that can enhance ourunder standing of hepatocarcinogenesis and develop individualized therapy based on HCC genetic signatures.

Supplementary Material

Refer to Web version on PubMed Central for supplementary material.

Acknowledgments

Financial Support

Funding was provided by the National Institutes of Health (U24CA143845 to G.G.), and the University Cancer Research Fund (D.Y.C.). D.Y.C. is the recipient of an Alfred P. Sloan Research Fellowship.

We wish to thank Bert O'Neil for a critical revision of this manuscript.

List of Abbreviations

DFS	Disease-free survival
HCC	hepatocellular carcinoma

References

1. Nault JC, Zucman-Rossi J. Genetics of hepatobiliary carcinogenesis. Semin Liver Dis. 2011; 31:173–187. [PubMed: 21538283]
2. Breuhahn K, Gores G, Schirmacher P. Strategies for hepatocellular carcinoma therapy and diagnostics: lessons learned from high throughput and profiling approaches. Hepatology. 2011; 53:2112–2121. [PubMed: 21433041]
3. Zender L, Villanueva A, Tovar V, Sia D, Chiang DY, Llovet JM. Cancer gene discovery in hepatocellular carcinoma. J Hepatol. 2010; 52:921–929. [PubMed: 20385424]
4. Moinzadeh P, Breuhahn K, Stutzer H, Schirmacher P. Chromosome alterations in human hepatocellular carcinomas correlate with aetiology and histological grade - results of an explorative CGH meta-analysis. Br J Cancer. 2005; 92:935–941. [PubMed: 15756261]
5. Patil MA, Gutgemann I, Zhang J, Ho C, Cheung ST, Ginzinger D, Li R, et al. Array-based comparative genomic hybridization reveals recurrent chromosomal aberrations and Jab1 as a potential target for 8q gain in hepatocellular carcinoma. Carcinogenesis. 2005; 26:2050–2057. [PubMed: 16000397]
6. Chiang DY, Villanueva A, Hoshida Y, Peix J, Newell P, Minguez B, Cozza A, et al. Focal *VEGFA* gains and molecular classification of hepatocellular carcinoma. 2008; 68:6779–6788.
7. Sieghart W, Losert D, Strommer S, Cejka D, Schmid K, Rasoul-Rockenschaub S, Bodingbauer M, et al. Mcl-1 overexpression in hepatocellular carcinoma: a potential target for antisense therapy. J Hepatol. 2006; 44:151–157. [PubMed: 16289418]
8. Chen L, Chan TH, Guan XY. Chromosome 1q21 amplification and oncogenes in hepatocellular carcinoma. Acta Pharmacol Sin. 2010; 31:1165–1171. [PubMed: 20676120]
9. Totoki Y, Tatsuno K, Yamamoto S, Arai Y, Hosoda F, Ishikawa S, Tsutsumi S, et al. High-resolution characterization of a hepatocellular carcinoma genome. Nat Genet. 2011; 43:464–469. [PubMed: 21499249]
10. Tao Y, Ruan J, Yeh SH, Lu X, Wang Y, Zhai W, Cai J, et al. Rapid growth of a hepatocellular carcinoma and the driving mutations revealed by cell-population genetic analysis of whole-genome data. Proc Natl Acad Sci U S A. 2011; 108:12042–12047. [PubMed: 21730188]
11. Li M, Zhao H, Zhang X, Wood LD, Anders RA, Choti MA, Pawlik TM, et al. Inactivating mutations of the chromatin remodeling gene ARID2 in hepatocellular carcinoma. Nat Genet. 2011; 43:828–829. [PubMed: 21822264]
12. Guichard C, Amaddeo G, Imbeaud S, Ladeiro Y, Pelletier L, Maad IB, Calderaro J, et al. Integrated analysis of somatic mutations and focal copy-number changes identifies key genes and pathways in hepatocellular carcinoma. Nat Genet. 2012; 44:694–698. [PubMed: 22561517]

13. Huang J, Deng Q, Wang Q, Li KY, Dai JH, Li N, Zhu ZD, et al. Exome sequencing of hepatitis B virus-associated hepatocellular carcinoma. Nat Genet. 2012; 44:1117–1121. [PubMed: 22922871]
14. Fujimoto A, Totoki Y, Abe T, Boroevich KA, Hosoda F, Nguyen HH, Aoki M, et al. Whole-genome sequencing of liver cancers identifies etiological influences on mutation patterns and recurrent mutations in chromatin regulators. Nat Genet. 2012; 44:760–764. [PubMed: 22634756]
15. Forbes SA, Bindal N, Bamford S, Cole C, Kok CY, Beare D, Jia M, et al. COSMIC: mining complete cancer genomes in the Catalogue of Somatic Mutations in Cancer. Nucleic Acids Res. 2011; 39:D945–950. [PubMed: 20952405]
16. Langmead B, Salzberg SL. Fast gapped-read alignment with Bowtie 2. Nat Methods. 2012; 9:357–359. [PubMed: 22388286]
17. McKenna A, Hanna M, Banks E, Sivachenko A, Cibulskis K, Kernytsky A, Garimella K, et al. The Genome Analysis Toolkit: a MapReduce framework for analyzing next-generation DNA sequencing data. Genome Res. 2010; 20:1297–1303. [PubMed: 20644199]
18. DePristo MA, Banks E, Poplin R, Garimella KV, Maguire JR, Hartl C, Philippakis AA, et al. A framework for variation discovery and genotyping using next-generation DNA sequencing data. Nat Genet. 2011; 43:491–498. [PubMed: 21478889]
19. Chapman MA, Lawrence MS, Keats JJ, Cibulskis K, Sougnez C, Schinzel AC, Harview CL, et al. Initial genome sequencing and analysis of multiple myeloma. Nature. 2011; 471:467–472. [PubMed: 21430775]
20. Banerji S, Cibulskis K, Rangel-Escareno C, Brown KK, Carter SL, Frederick AM, Lawrence MS, et al. Sequence analysis of mutations and translocations across breast cancer subtypes. Nature. 2012; 486:405–409. [PubMed: 22722202]
21. Wang K, Li M, Hakonarson H. ANNOVAR: functional annotation of genetic variants from high-throughput sequencing data. Nucleic Acids Res. 2010; 38:e164. [PubMed: 20601685]
22. Seal RL, Gordon SM, Lush MJ, Wright MW, Bruford EA. genenames. org: the HGNC resources in 2011. Nucleic Acids Res. 2011; 39:D514–519. [PubMed: 20929869]
23. Livak KJ, Schmittgen TD. Analysis of relative gene expression data using real-time quantitative PCR and the 2(-Delta Delta C(T)) Method. Methods. 2001; 25:402–408. [PubMed: 11846609]
24. Ding L, Getz G, Wheeler DA, Mardis ER, McLellan MD, Cibulskis K, Sougnez C, et al. Somatic mutations affect key pathways in lung adenocarcinoma. Nature. 2008; 455:1069–1075. [PubMed: 18948947]
25. Copple IM, Lister A, Obeng AD, Kitteringham NR, Jenkins RE, Layfield R, Foster BJ, et al. Physical and functional interaction of sequestosome 1 with Keap1 regulates the Keap1-Nrf2 cell defense pathway. J Biol Chem. 2010; 285:16782–16788. [PubMed: 20378532]
26. Li CQ, Kim MY, Godoy LC, Thiantanawat A, Trudel LJ, Wogan GN. Nitric oxide activation of Keap1/Nrf2 signaling in human colon carcinoma cells. Proc Natl Acad Sci U S A. 2009; 106:14547–14551. [PubMed: 19706542]
27. Taguchi K, Motohashi H, Yamamoto M. Molecular mechanisms of the Keap1-Nrf2 pathway in stress response and cancer evolution. Genes Cells. 2011; 16:123–140. [PubMed: 21251164]
28. Sung WK, Zheng H, Li S, Chen R, Liu X, Li Y, Lee NP, et al. Genome-wide survey of recurrent HBV integration in hepatocellular carcinoma. Nat Genet. 2012; 44:765–769. [PubMed: 22634754]
29. Lee J, Kim DH, Lee S, Yang QH, Lee DK, Lee SK, Roeder RG, et al. A tumor suppressive coactivator complex of p53 containing ASC-2 and histone H3-lysine-4 methyltransferase MLL3 or its paralogue MLL4. Proc Natl Acad Sci U S A. 2009; 106:8513–8518. [PubMed: 19433796]
30. Ansari KI, Kasiri S, Mishra BP, Mandal SS. Mixed lineage leukaemia-4 regulates cell-cycle progression and cell viability and its depletion suppresses growth of xenografted tumor in vivo. Br J Cancer. 2012; 107:315–324. [PubMed: 22713656]
31. Woo HG, Wang XW, Budhu A, Kim YH, Kwon SM, Tang ZY, Sun Z, et al. Association of TP53 mutations with stem cell-like gene expression and survival of patients with hepatocellular carcinoma. Gastroenterology. 2011; 140:1063–1070. [PubMed: 21094160]
32. Villanueva A, Llovet JM. Targeted therapies for hepatocellular carcinoma. Gastroenterology. 2011; 140:1410–1426. [PubMed: 21406195]
33. Zhu AX. Molecularly targeted therapy for advanced hepatocellular carcinoma in 2012: current status and future perspectives. Semin Oncol. 2012; 39:493–502. [PubMed: 22846866]

34. Mok TS, Wu YL, Thongprasert S, Yang CH, Chu DT, Saijo N, Sunpaweravong P, et al. Gefitinib or carboplatin-paclitaxel in pulmonary adenocarcinoma. N Engl J Med. 2009; 361:947–957. [PubMed: 19692680]

35. McArthur GA, Puzanov I, Amaravadi R, Ribas A, Chapman P, Kim KB, Sosman JA, et al. Marked, homogeneous, and early [18F]fluorodeoxyglucose-positron emission tomography responses to vemurafenib in BRAF-mutant advanced melanoma. J Clin Oncol. 2012; 30:1628–1634. [PubMed: 22454415]

36. Hoshida Y, Villanueva A, Kobayashi M, Peix J, Chiang DY, Camargo A, Gupta S, et al. Gene expression in fixed tissues and outcome in hepatocellular carcinoma. N Engl J Med. 2008; 359:1995–2004. [PubMed: 18923165]

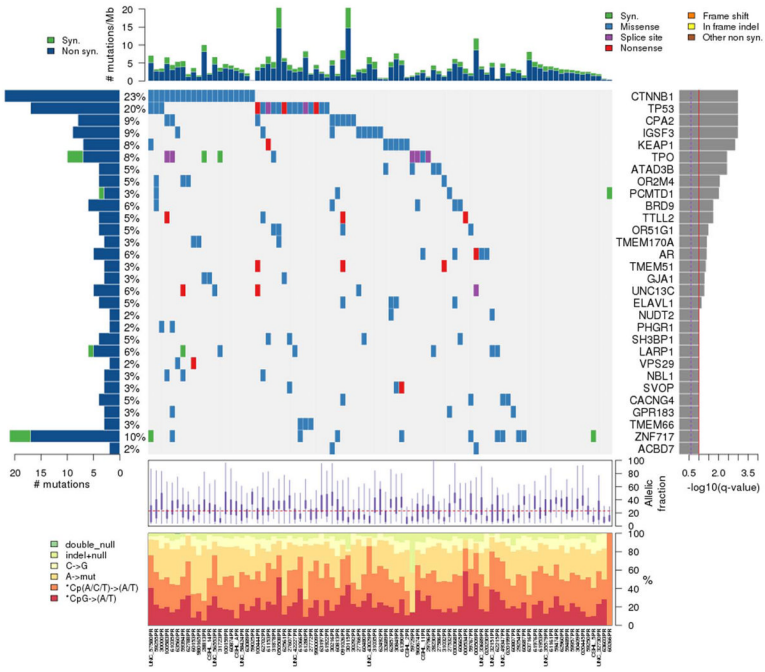

Figure 1. Mutation landscape of 87 hepatocellular carcinomas

The matrix in the center of the figure represents individual mutations in patient samples, color-coded by type of mutation, for the significantly mutated genes. The rate of synonymous and non-synonymous mutations is displayed at the top of the matrix. The barplot on the left of the matrix shows the number of mutations in each gene. The percentages represent the fraction of tumors with at least one mutation in the specified gene. The barplot to the right of the matrix displays the q-values for the most significantly mutated genes. The purple boxplots below the matrix represent the distributions of allelic fractions observed in each sample. The plot at the bottom represents the base substitution distribution of individual samples, using the same categories that were used to calculate significance.

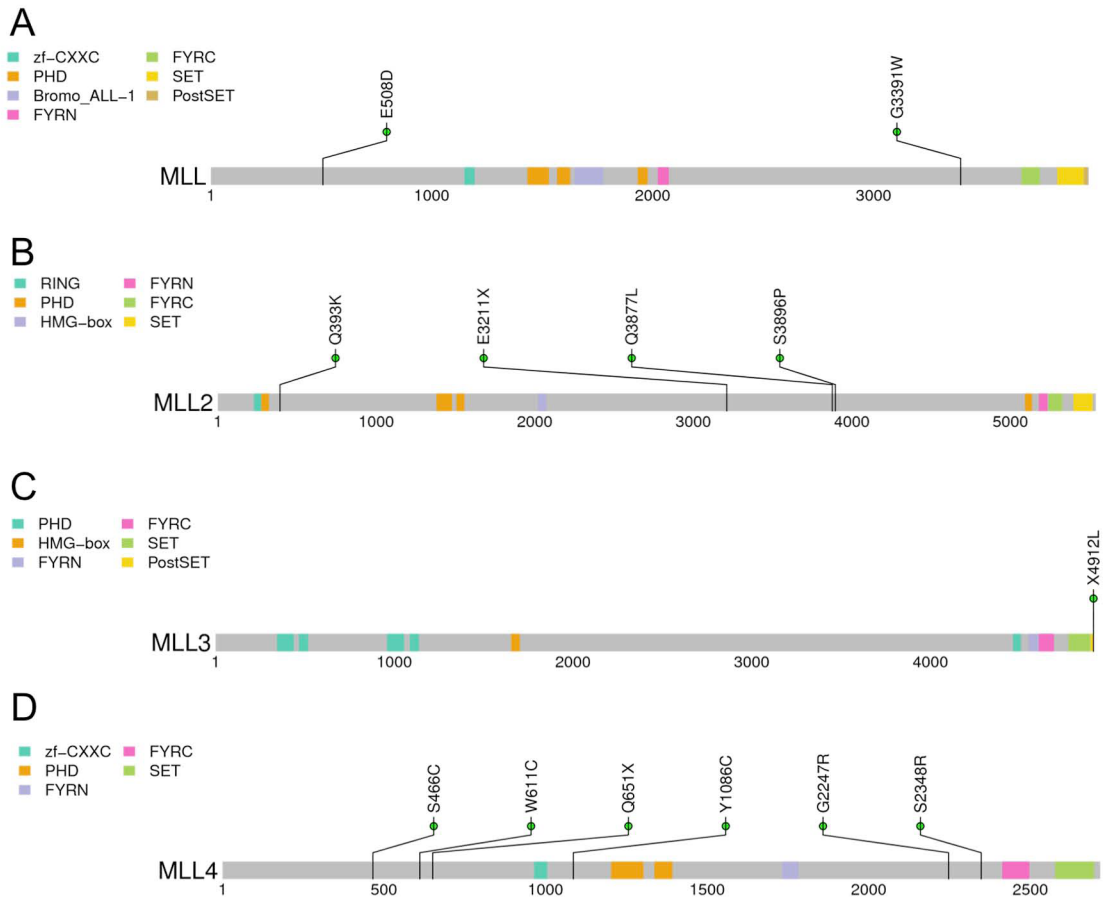

Figure 2. Protein domain structure of histone methyltransferases

Mutations are displayed at the protein coding residues, and protein domains are indicated by the colored blocks.

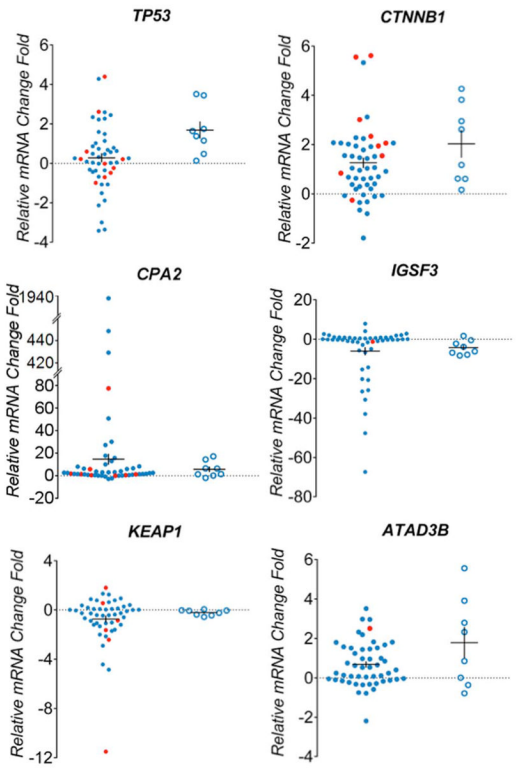

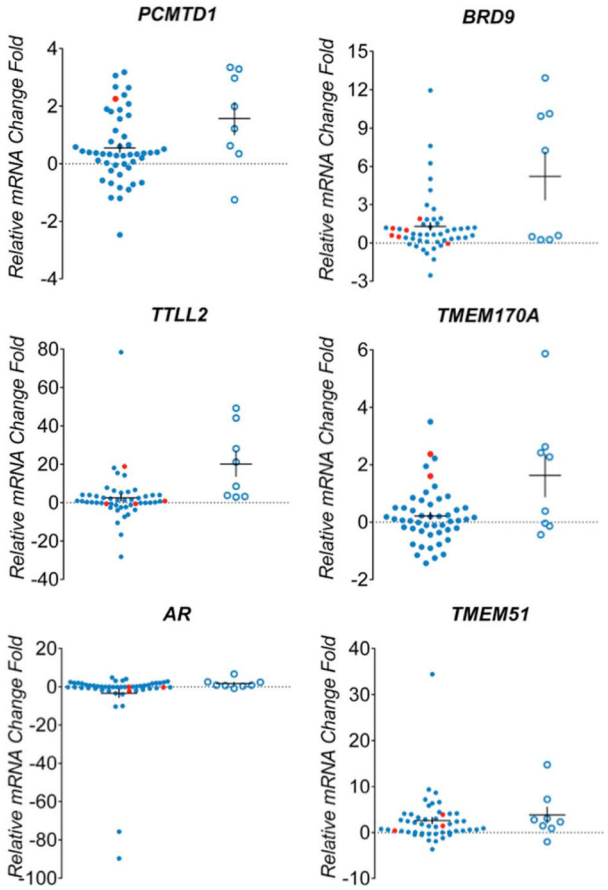

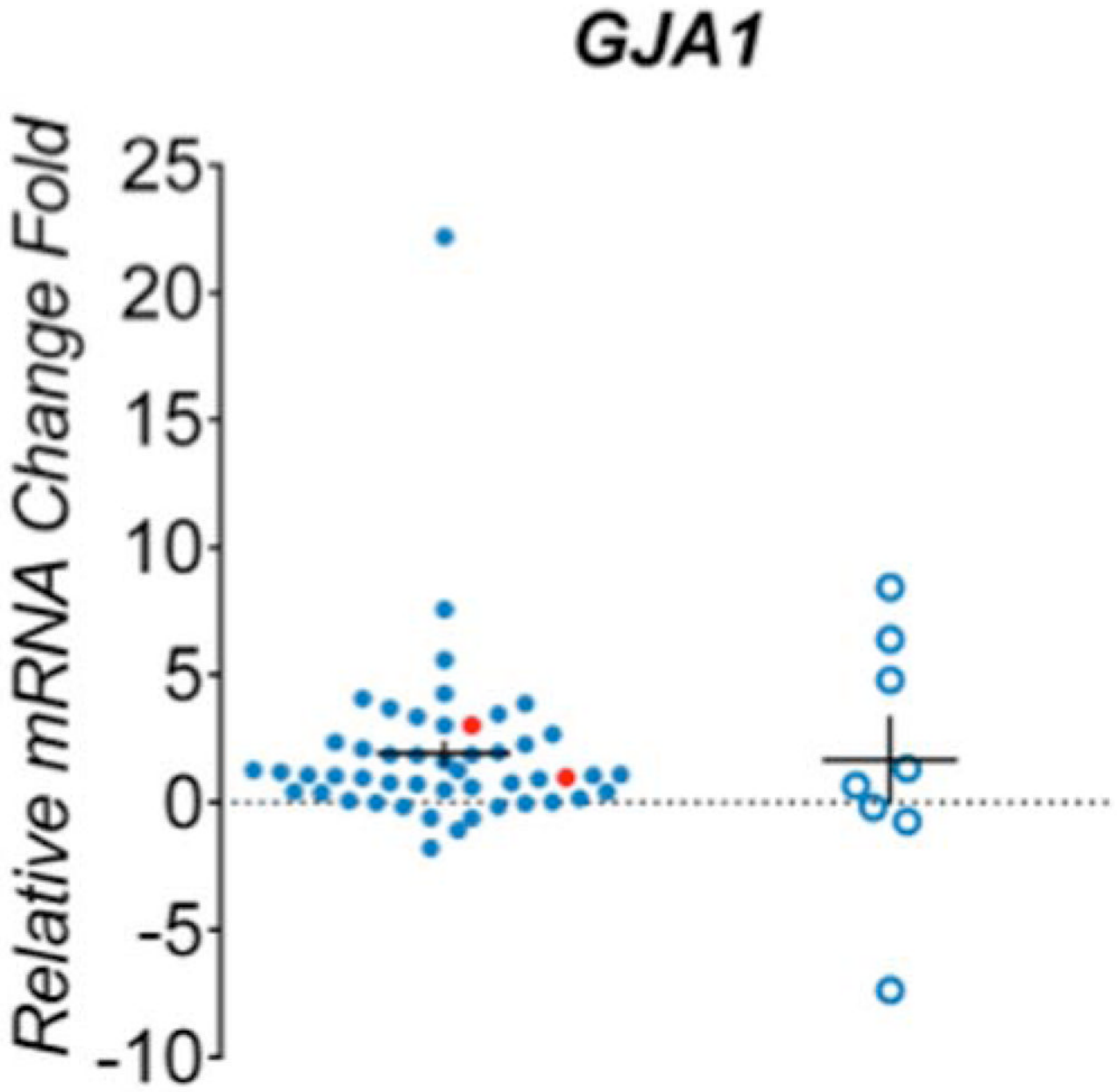

Figure 3. Expression levels of mutated genes in hepatocellular carcinomas

Real-time PCR analysis of 13 genes differentially expressed among 49 HCC tumors(blue dot) and 8 adjacent tissues (blue circle). Samples confirmed with target gene mutation were highlighted in red. The mRNA expression level was normalized to zero based on normal human liver samples. The vertical axis indicates the relative increase (+) or decrease (−) fold-change of each tumor or adjacent sample compared with normal human liver.

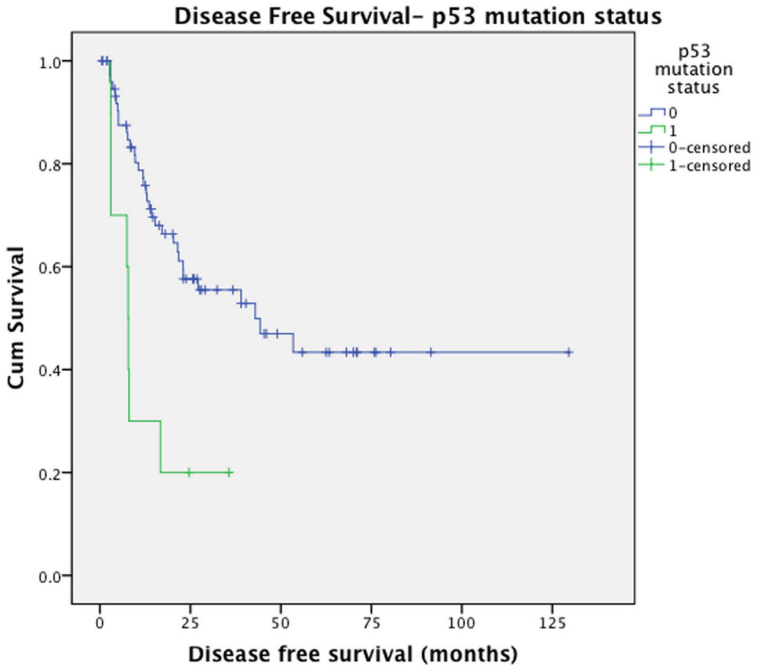

Figure 4.
Disease-free survival according to p53 mutation status.

Table 1

Clinical characteristics of HCC samples.

	Patients N=87(%)
Male: Female	61(77):18(23)
Median Age (range)	61 (16–83)
Predisposing etiology*	
HBV	38(43)
HCV	19(21)
Alcohol	10(11)
Hemochromatosis	3(3)
Cirrhosis	49 (56)
Tumor Number	
1	69(78)
2–3	15(17)
≥4	4(5)
Median tumor size (range)	6.2 (2–18)
Pathology Characteristics	
CK19 positive	12 (14)
Fibrolamellar HCC	2(2)
Tumor rupture	2(2)
Grade	
Well differentiated	6(7)
Moderately differentiated	66(75)
Poorly differentiated	16(18)
Edmonson-Steiner Grade	
1	5(5)
2	21(24)
3	49(56)
4	13(15)
Vascular invasion	
Microvascular	44(50)
Macrovascular (large vessel)	12(14)

*-patients may have more than one predisposing condition

Table 2

Significantly mutated genes in 87 hepatocellular carcinomas

Gene	Description	# patients	# sites	Mutation significance (FDR *q*-val)
CTNNB1	Beta-catenin	20	14	$<1 \times 10^{-11}$
TP53	Tumor protein p53	17	14	$<1 \times 10^{-11}$
CPA2	Carboxypeptidase A2 (pancreatic)	8	2	3.22×10^{-6}
IGSF3	Immunoglobulin superfamily, member 3	8	5	1.3×10^{-5}
KEAP1	Kelch-like ECH-associated protein 1	7	7	4×10^{-4}
ATAD3B	ATPase, AAA domain containing 3B	4	2	2.6×10^{-3}
PCMTD1	protein-L-isoaspartate (D-aspartate) O- methyltransferase domain containing 1	3	2	8.3×10^{-3}
BRD9	Bromodomain containing 9	5	2	0.017
TTLL2	Tubulin tyrosine ligase-like family, member 2	4	2	0.017
TMEM170A	Transmembrane protein 170A	3	1	0.037
AR	Androgen receptor	5	5	0.038
TMEM51	Transmembrane protein 51	3	1	0.042
GJA1	Gap junction protein, alpha 1, 43kDa	3	3	0.049

Table 3

Significantly mutated gene families in 87 hepatocellular carcinomas

Symbol	Family description	# genes	Mutation rate in family	t-test (rate)
NLR	Nucleotide-binding domain and leucine rich repeat containing	22	2.68E-06	0.0033
MLL	Mixed lineage leukemia histone methyltransferases	5	2.85E-06	0.0037
CACN	Calcium channel subunits	26	2.17E-06	0.0041
KMT	Chromatin-modifying enzymes/K-methyltransferases	26	2.13E-06	0.0060

Table 4

Predictors of disease-free survival (DFS)

	Median DFS months (95%CI)	Univariate Analysis[1]	Multivariate analysis HR[2] (95%CI), p-value
P53		P=0.001	
No mutation	42.9 (14–72)		4.2 (1.9- 9.7), p=0.02
Mutation (+)	7.9 (7.2–8.5)		
MLL		P=0.38	
No mutation	42.9 (6.1–79.8)		
Mutation (+)	23.1 (3.9–42.2)		
B-catenin		P=0.51	
No mutation	27.1 (4.9–49.3)		
Mutation (+)	43.0 (1–99.1)		
CPA2		P=0.25	
No mutation	42.9 (20.4–65.5)		
Mutation (+)	15.3 (5.3–25.2)		
Age		P=0.16	
Tumour Number		P=0.08	
Solitary	44.3 (10.3–78.3)		2.0(0.97–4.1), p=0.06
Multifocal	15.4 (3.0–27.3)		
Tumour Size		P=0.04	1.04(0.9–1.08), p=0.08
HBV		P=1.0	
Negative	27.1 (1–53.4)		
Positive	44.3 (32.1–56.5)		
HCV		P=0.91	
Negative	39.0 (15.2–62.9)		
Positive	27.1 (10–44.2)		
Tumour Grade		P=0.83	
Well diff	39.0 (5.2–72.8)		
Moderately diff	32.9 (14.5–71.5)		
Poorly diff	21.5 (9.7–33.2)		
Microvascular Inv.		P=0.19	
Negative	44.3 (12.8–75.7)		
Positive	21.8 (9.6–33.9)		

[1] Log-rank test

[2] Hazard ratio by Cox proportional hazards model